5

Finite element simulation. Applications in Orthopaedic Surgery and Traumatology

Antonio Herrera[a,c], Luis Gracia[b], Elena Ibarz[b], Juan J. Panisello[a,c], José Cegoñino[b], Jesús Mateo[a,c], Javier Rodríguez-Vela[a,c] and Sergio Puértolas[b]
[a]*Medicine School. University of Zaragoza (Spain)*
[b]*Engineering Faculty. University of Zaragoza (Spain)*
[c]*Miguel Servet University Hospital, Zaragoza (Spain)*

1. Introduction

Research in different fields concerning Orthopaedic Surgery and Traumatology requires a methodology that allows, at the same time, a more economic approach and the possibility of reproducing in a easy way different situations. Such a method could be used as a guide for research on biomechanics of the locomotor system, both in healthy and pathologic conditions, along with the study of performance of different prostheses and implants. To that effect, the use of simulation models, introduced in the field of Bioengineering in recent years, can undoubtedly mean an essential tool to assess the best clinical option, provided that it will be accurate enough in the analysis of specific physiological conditions concerning a certain pathology.

The Finite Element Method (FEM) was originally developed for solving structural analysis problems relating to Mechanics, Civil and Aeronautical Engineering. The paternity of this method is attributed to Turner, who published his first, historic, job in 1956 (Turner et al., 1956). In 1967 Zienkiewicz OC published the book "The finite element method in structural and continuum mechanics" (Zienkiewicz, 1967) which laid down mathematical basis of the method. Other fundamental contributions to the development of Finite Element Method (FEM) took place on dates nearest (Imbert, 1979; Bathe, 1982; Zienkiewicz & Morgan, 1983; Hughes, 1987).

Finite element (FE) simulation has proved to be specially suitable in the study of the behaviour of any physiological unit, despite its complexity. Nowadays, it has become a powerful tool in the field of Orthopaedic Surgery and Traumatology, helping the surgeons to have a better understanding of the biomechanics, both in healthy and pathological conditions. FE simulation let us know the biomechanical changes that occur after prosthesis or osteosynthesis implantation, and biological responses of bone to biomechanical changes. It also has an additional advantage in predicting the changes in the stress distribution around the implanted zones, allowing to prevent future pathologies derived from an unsuitable positioning of the prostheses or its fixation. Simulation also allows us to predict the behavior of orthopedic splints, utilized for the correction of deformities, providing the

recovering force-displacement and angle-moment curves that characterize the mechanical behavior of the splint in the overall range of movement.

2. Methology for the finite element analysis of biomechanical systems

One of the most significant aspects of biomechanical systems is its geometric complexity, which greatly complicates the generation of accurate simulation models. Classic models just suffered from this lack of geometrical precision, present even in recent models (Guan et al., 2006; Little et al., 2007), which challenged, in most studies, the validity of the results and their extrapolation to clinical settings.

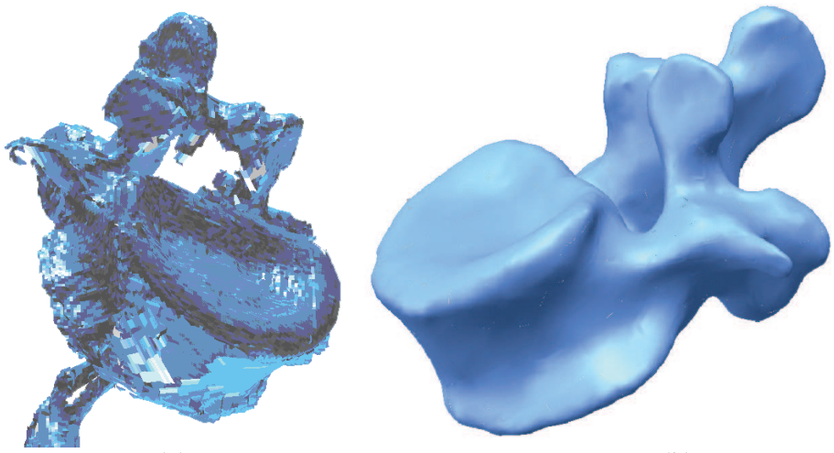

(a) (b)

Fig. 1. 3D scanning of a vertebra: a) Original without processing; b) Final after processing

Fig. 2. 3D laser scanner

Fig. 3. Anatomical model of the lumbar spine

Currently, there are methodologies developed over recent years that avoid such problems, allowing the generation of models with the desired precision in a reasonable time and cost is not excessive. Thus, the use of scanners together with three-dimensional images obtained by CT allow making geometric models that combine high accuracy in the external form with an excellent definition of internal interfaces. The method requires not only appropriate software tools, capable of processing images, but also its compatibility with the programs used later to generate the finite element model. For example, in Fig. 1a is shown the initial result obtained by a three-dimensional laser scanner Roland Picza (Fig. 2), from an anatomical model of the lumbar spine Somso brand QS-15 (Fig. 3).
After processing by Dr. Picza 3 and 3D Editor programs, we get the final result in Fig. 1b, which shows the geometric precision obtained. In these models, the characterization of the internal structure is made by 3D CT, from images like that shown in Fig. 4. An alternative to the above procedure is the use of 3D geometrical reconstruction programs, for example, MIMICS (Mimics, 2010). In any case, the final result is a precise geometrical model which serves as a basis for the generation of a finite elements mesh.

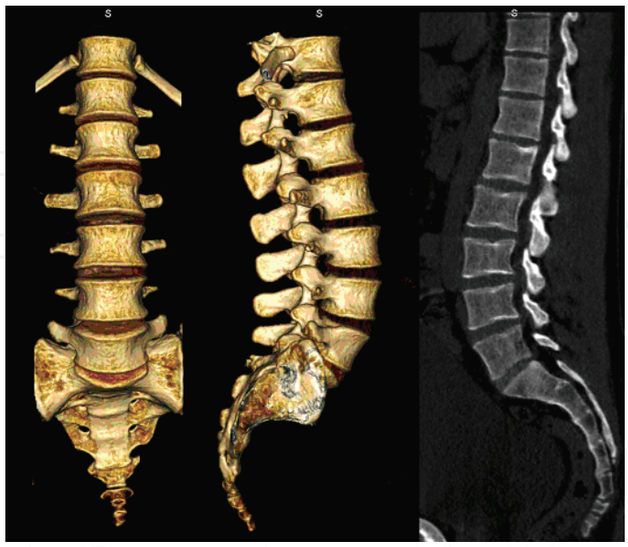

Fig. 4. Volume rendering 3D reconstruction and sagital multiplanar reconstruction of the lumbar spine

In view of the difficulties experienced in living subjects, FE simulation models have been developed to carry out researches on biomechanical systems with high reproducibility and versatility. These models allow to repeat the study as many times as desired, being a non-aggressive investigation of modified starting conditions. However, work continues on the achievement of increasingly realistic models that allow to put the generated results and predictions into a clinical setting. To that purpose it is mainly necessary the use of meshes suitable for the particular problem, as regards both the type of elements and its size. It is always recommended to perform a sensitivity analysis of the mesh to determine the optimal features or, alternatively, the minimum necessary to achieve the required accuracy. In Fig. 5 is shown a FE mesh of a lumbar vertebral body, using tetrahedron type elements. It can be seen that the element size allows to depict, with little error, the geometry of the vertebra, compared with Fig. 1b.

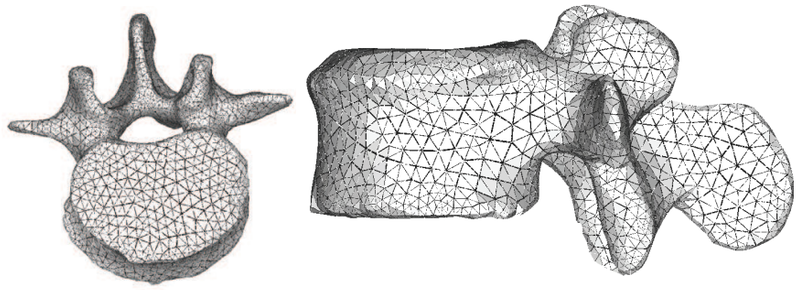

Fig. 5. Meshing of a lumbar vertebra

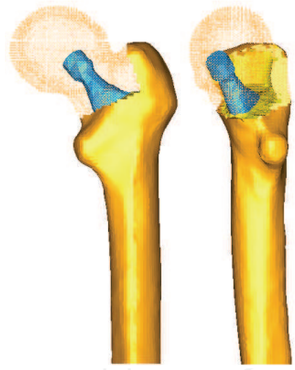

Fig. 6. Meshing of proximal fémur with stem

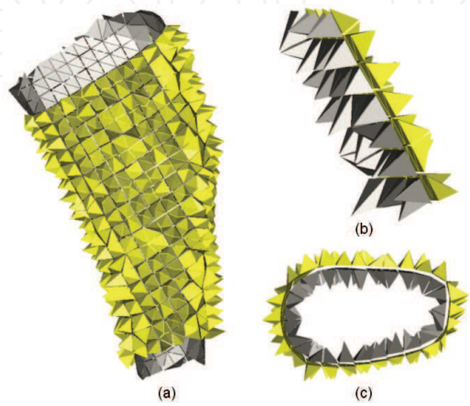

Fig. 7. Contact interface femur-stem

A key issue in FE models is the interaction between the different constitutive elements of the biomechanical system, especially when it comes to conditions which are essential in the behaviour to be analyzed. Thus, in Fig. 6 is shown a FE mesh of the proximal femur, with a cementless stem in place. The biomechanical behaviour of this type of implant depends basically on the conditions of contact between the stem and bone, so that the correct simulation of the latter determines the validity of the model. In Fig 7 can be seen the stem-femur contact interface, defined by the respective surfaces and the frictional conditions needed to produce the press-fit which is achieved at surgery.
Finally, in FE simulation models is essential the appropriate characterization of the mechanical behaviour of the different materials, usually very complex. So, the bone exhibits an anisotropic behaviour with different responses in tension and compression (Fig. 8). Moreover, it varies depending on the bone type (cortical or cancellous) and even along different zones in the same specimen, as in the vertebrae (Denozière & Ku, 2006). This kind of behaviour is reproducible in a reliable way in the simulation, but it leads to an excessive computational cost in global models. For this reason, in most cases, and specially in long bones, a linear elastic behaviour in the operation range concerning strains and stresses is considered.

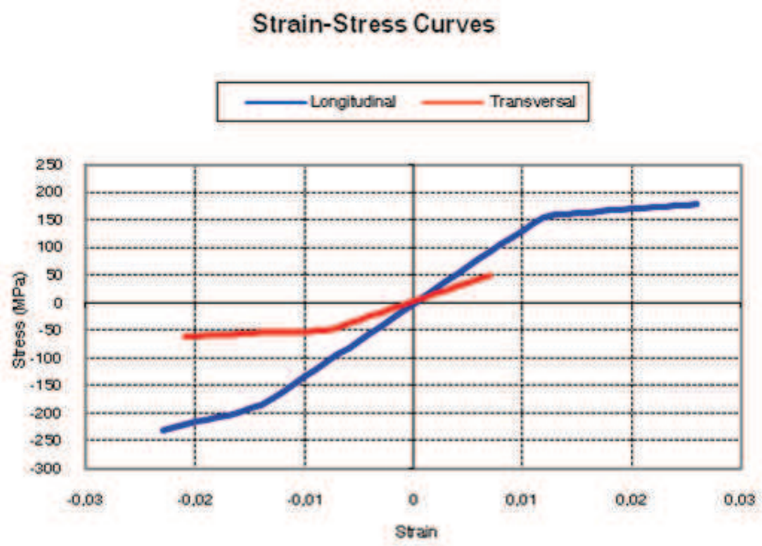

Fig. 8. Strain-stress curves for cortical bone

In soft tissues, the behaviour is even more complex, usually as a hyperelastic material. This is the case of ligaments (Fig. 9), cartilages and muscles, also including a reologic effect with deferred strains when the load conditions are maintained (viscoelastic behaviour). A special case arises in the intervertebral discs, where nucleus and annulus present totally different features: while the nucleus behaves as an incompressible fluid, the annulus could be considered as a two-phase material with a flexible matrix and a set of fibers with only tension hyperelastic behaviour.
This inherent complexity to the different biological tissues, reproducible in reduced or local models, is very difficult to be considered in global models as the used to analyse prostheses and implants, because the great amount of non-linearities do the convergence practically

unfeasible. On the other hand, it leads to a prohibitive computational cost, only possible to undertake by supercomputers.

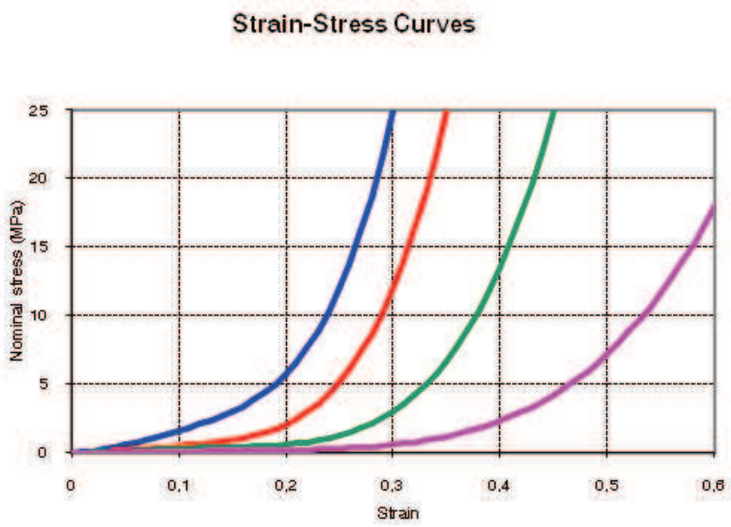

Fig. 9. Strain-stress curves for vertebral ligaments

3. Application to the behaviour of hip prostheses

Bone is living tissue that undergoes a constant process of replacement of its structure, characterized by bone reabsorption and new bone formation, without changing their morphology. This process is called bone remodeling. On the other hand, bone adapts its structure, according to Wolff's Law, to the forces and biomechanical loads that receives (Buckwalter et al., 1995). In a normal hip joint, loads from the body are transmitted to the femoral head, then to the medial cortical bone of femoral neck towards the lesser trochanter, where they are distributed by the diaphyseal bone (Radin, 1980).

The implantation of a cemented or cementless femoral stem produced a clear alteration of the physiological transmission of loads, as these are now passed through the prosthetic stem, in a centripetal way, from the central marrow cavity to the cortical bone (Marklof et al., 1980). These changes of the normal biomechanics of the hip bone leads to a phenomenon called adaptive remodeling (Huiskes et al., 1989), since bone has to adapt to the new biomechanical situation. Remodeling is a multifactorial process depending on both mechanical and biological factors. Mechanical factors are related to the new distribution of loads caused by implantation of the prosthesis in the femur, the physical characteristics of the implant (size, implant design and alloy), and the type of anchoring in the femur: metaphyseal, diaphyseal, hybrid, etc. (Summer & Galante, 1992; Sychter & Engh, 1996; Rubash et al., 1998; McAuley et al., 2000; Gibson et al., 2001; Glassman et al., 2001). Biologics are related to age and weight of the individual, initial bone mass, quality of primary fixation and loads applied to the implant. Of these biological factors, the most important is initial bone mass (Sychter & Engh, 1996).

Different models of cementless stems have tried to achieve perfect load transfer to the femur, mimicking the physiological transmission from the femoral calcar to the femoral shaft. The main objective was to avoid stress-shielding, since in absence of physiological transmission of loads, and lack of mechanical stimulus in this area, causes a proximal bone atrophy.

Cemented stem fixation is achieved by the introduction of cement into bone, forming a bone-cement interface. Inside the cement mantle a new interface is made up between cement and stem. It might seem that the cement mantle enables better load distribution in the femur; however the design, material and surface of prostheses, play an important role in transmission and distribution of charges, influencing bone remodelling (Ramaniraka et al., 2000; Li et al., 2007)
Long-term follow-up of different models of cementless stems have shown that this is not achieved, and to a greater or lesser extent the phenomenon of stress-shielding is present in all the models, and therefore the proximal bone atrophy. It is interesting to know, in cemented stems, not only the stress-shielding and subsequent proximal bone atrophy, but also the long-term behavior of cement-bone and stem-cement interfaces. This requires long-term studies monitoring the different models of stems.
FE simulation allows us to study the long term biomechanical behavior of any type of stem cemented or cementless, and predict the impact of biomechanics on the femur, with its consequent effects on bone remodelling . So, we have developed FE models to study the biomechanical behavior of cemented and cementless stems. Our models have been validated with long-term DEXA studies of patients who were treated with different types of femoral stems (Herrera et al., 2007; Herrera et al., 2009).
The development of the model of a healthy femur is crucial to make accurate the whole process of simulation, and to obtain reliable results. A femur from a 60 years old man, died in traffic accident, has been used to build the model. Firstly, each of the parts necessary to set the final model were scanned using a three dimensional scanner Roland Picza brand. As a result, we get a cloud of points which approximates the scanned geometry. These surfaces must be processed through the programs Dr.Picza-3 and 3D-Editor. This will eliminate the noise and performs smooth surfaces, resulting in a geometry that reliably approximates to the actual geometry .

(a) (b)
Fig. 10. a) FE model of healthy femur, b) Coronal section of healthy femur model

CT scans and 3D-CT reconstructions were taken from the femur to determine the geometry of the cancellous bone, allowing a perfect model of this part of the bone. For a precise geometry, splines are plotted according to the tomograms and then the cancellous surface is

modelled. This area represents the separation between cortical and cancellous bone. The meshing is performed by using I-deas program (I-deas, 2007), which creates two groups of elements (cancellous and cortical). Taking cancellous bone elements as start point, a third group of elements is selected by applying the properties of bone marrow. The mesh is based on tetrahedral solid elements with linear approximation, obtaining a total of 408,518 elements (230,355 elements for cortical bone, 166,220 elements for cancellous bone and 11,943 elements for bone marrow) (Fig. 10).
Different publications (Evans, 1973) were consulted to obtain the properties of bone material. Table 1 summarizes the mechanical properties values used in biological materials, which have been simplified to consider bone as isotropic and linear elastic material.

MATERIAL	ELASTIC MODULUS (MPa)	POISSON RATIO	MAXIMUM COMPRESSION STRESS (MPa)	MAXIMUM TENSION STRESS (MPa)
CORTICAL BONE	20000	0,3	150	90
CANCELLOUS BONE	959	0,12	23	
BONE MARROW	1	0,3		

Table 1. Mechanical properties of the healthy femur model

The main features of each of the boundary conditions are:

1.- Clamped in the middle of the femoral shaft

The middle zone has been clamped instead of distal zone because middle zone is considered enough away from proximal bone (Fig. 11). This model can be compared with other that have been clamped at a distal point, since the loads applied practically coincided with the femoral axis direction thus reducing the differences in final values.

2.- Hip muscles Loads

Forces generated by the abductor muscles are applied on the greater trochanter, in agreement with most authors' opinion (Weinans et al., 1994; Kerner et al., 1999). Generally, muscle strength generated in the hip joint is 2 times the body weight, and this produces a reaction strength in the femoral head that accounts for 2.75 times the body weight. However, when the heel impacts to the ground, and in double support stage of the gait, the load increases up to 4 times the body weight. The latter case, being the worst one, has been considered to impose the boundary conditions. It has also been considered a body weight of 79.3 kg for cementless stems, and 73 kg for cemented stems. Those were the average values obtained from the clinical sample to be contrasted with the simulation results. The load due to the abductor muscles, accounting for 2 times the corporal weight, is applied to the proximal area of the greater trochanter, at an angle of 21 degrees, as shown in Fig. 11.

3.- Reaction strength on the femoral head due to the body weight.

As already mentioned, we have studied the case of a person to 79.3 kg in cementless stems, and 73 kg in cemented stems, in the worst case of double support or heel impact stages of

the gait. The resultant force on the femoral head would be worth 4 times the body weight (Fig. 11).

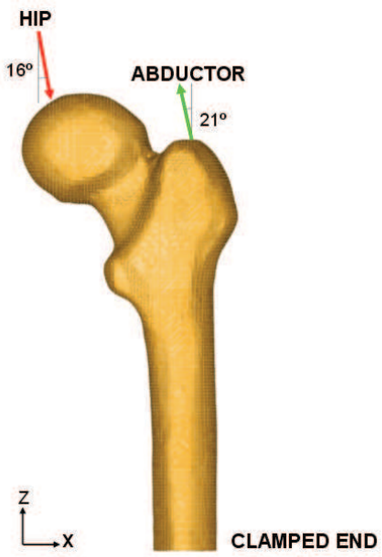

Fig. 11. Boundary conditions applied in the healthy femur model

The models generated using I-deas are calculated by means of Abaqus 6.7, and the postprocessing of the results was performed by Abaqus Viewer (Abaqus, 2009).

To generate the models from different stems, these were scanned to obtain its geometry. We studied two cementless stems. Both of them were anatomically shaped, metaphyseal anchored and coated with HA in their metaphyseal zone (ABG I and ABG II). The size used has been similar in both models, however the alloy, geometry, length, thickness and distal diameter were different. For cemented stems models, we chose the cemented anatomical stem ABG, and the Versys straight, polished stem. After obtaining the geometry of the different stems, several cadaver femurs were operated on in order to implant each of the prostheses, in the same way as one would carry out a real hip replacement.

Those operated femurs were scanned a second time to use them as a reference in the positioning of the prostheses. We employ, for every model, three meshes generated by the I-deas program: healthy femur, femoral stem, and operated femur. The mesh of healthy femur and the mesh of the operated femur were superimposed, then the healthy femoral epiphysis was removed in a identical way as it is done during surgery, so as to insert the prosthesis. Afterward the stem was positioned in the femur, always taking the superimposed mesh of the operated femur as a base (Fig. 12).

In the case of cementless stems, the previous process for modeling the cadaveric femur was repeated only for cortical bone. While the cancellous bone was modeled again in such a way that it fitted perfectly to contact with the prostheses. The Abaqus 6.7 program was utilized for calculation and simulation of the previously generated models, and the Abaqus Viewer was used for viewing the results. Union between the stems and the cancellous bone were not considered, but contact conditions were defined with a constant 0.5 friction coefficient, simulating the perfect press-fit setting. The final model with ABG-I stem comprises a total of 60401 elements (33504 for cortical bone, 22088 for cancellous bone and 4809 for ABG-I stem). The final model with the ABG-II stem is made up of 63784 elements (33504 for cortical bone,

22730 for cancellous bone and 7550 for ABG-II stem). Fig. 13 shows both FE models obtained for cementless prostheses.

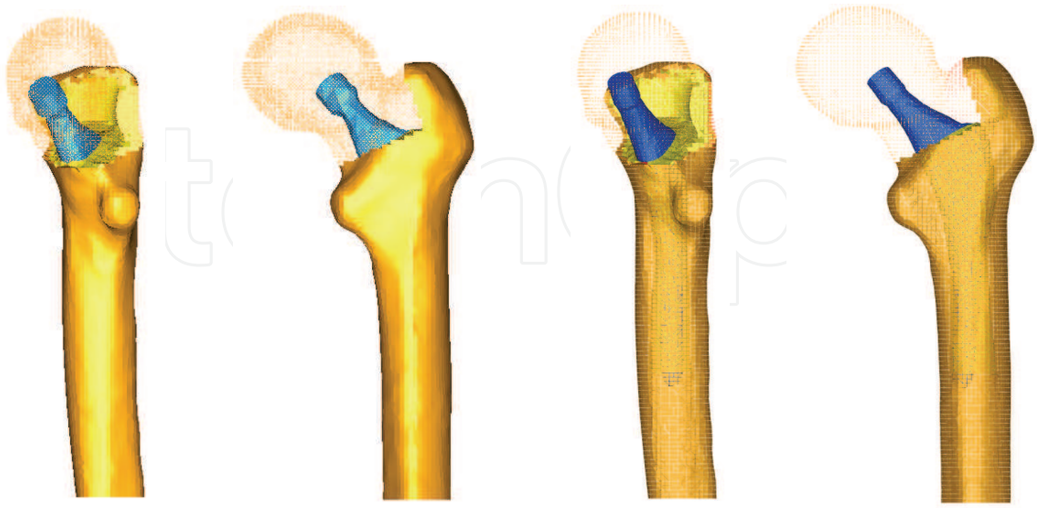

(a) (b)

Fig. 12. Removal of the femoral head and positioning of the cementless stems: (a) ABG-I and (b) ABG-II.

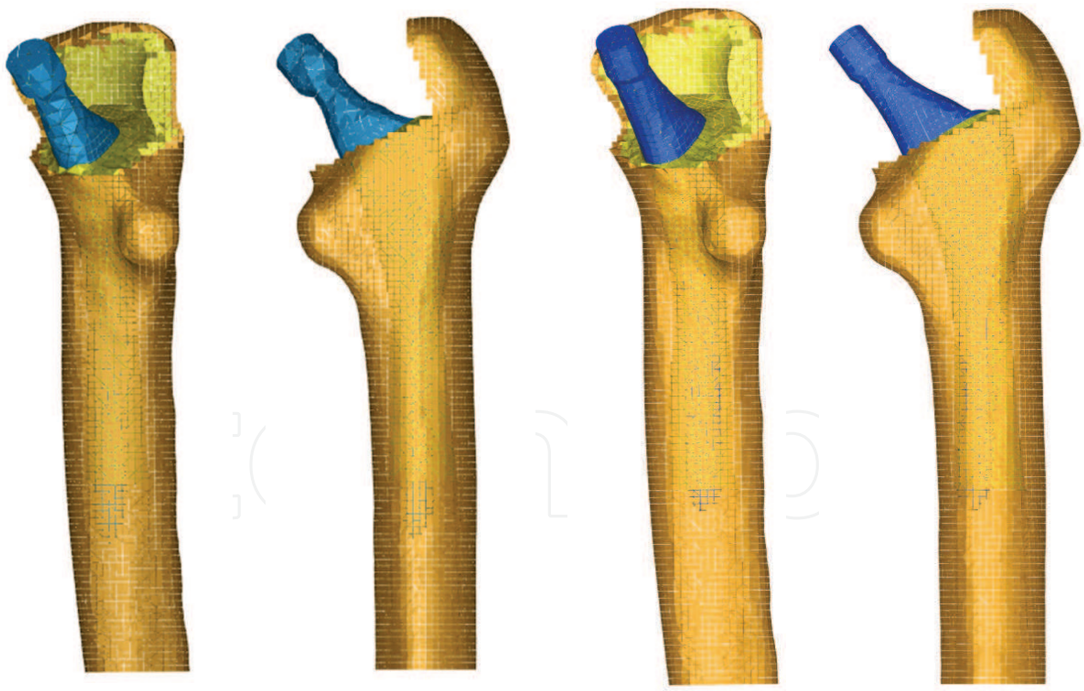

(a) (b)

Fig. 13. FE models of the femur with cementless prosthesis: (a) ABG-I and (b) ABG-II

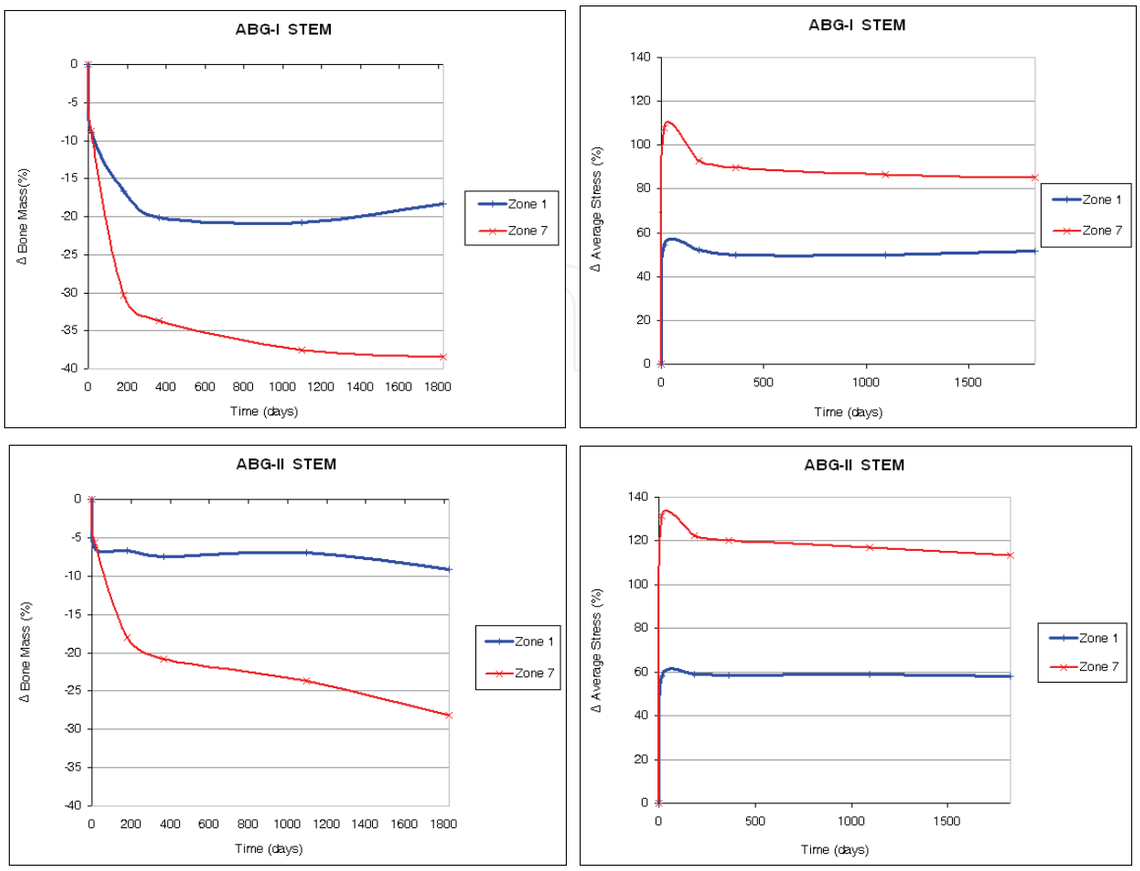

Fig. 14. BMD and average von Mises stress evolution

Calculation was performed using the program Abaqus 6.7. Both prostheses have been simulated with the same mechanical properties, thus, the result shows the influence of stem geometry on the biomechanical behavior. Fig. 14 shows, for each cementless stem model, the change (%) in BMD and average von Mises stress corresponding to the Gruen proximal zones (1 and 7), being the most representative concerning stress-shielding, and taking as reference the pre-operative data. It can be confirmed, for both stems, that the maximum devreasing in BMD is achieved in zone 7. This reduction in BMD is bigger in the ABG-I than in ABG-II stem.

In the case of cemented stems the process of modelling was similar, varying the surgical cut in the femoral neck of the healthy femur. Each stem was positioned into the femur, always taking the superimposed mesh of the operated femur as a base (Fig. 15). In the previous process of modelling, on the cadaveric femur, only the cortical bone was used. The cancellous bone was modelled again taking into account the cement mantle surrounding the prosthesis and the model of stem (ABG or Versys), so as to obtain a perfect union between cement and cancellous bone. The cement mantle was given a similar thickness, in mm, which corresponds to that usually achieved in patients operated on, different for each of the stem models studied and each of the prosthesis, so that the simulation model be as accurate as possible.

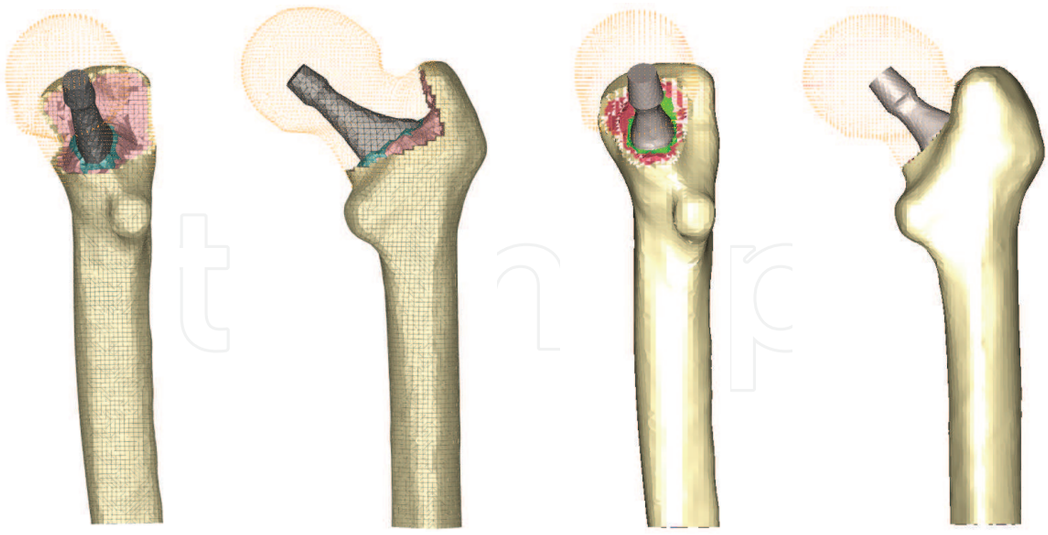

(a) (b)

Fig. 15. Removal of the femoral head and cemented prosthesis positioning: (a) ABG-cemented and (b) Versys

In models of cemented prostheses it is not necessary to define contact conditions between the cancellous bone and the stem. In this type of prosthesis the junction between these two elements is achieved by cement, which in the EF model should simulate conditions of perfect union between cancellous bone-cement and cement-stem. It has also been necessary to model the diaphyseal plug that is placed in actual operations to prevent the spread of the cement down to femoral medullary canal. Fig. 16 shows the longitudinal sections of the final models.

(a) (b)

Fig. 16. Longitudinal section of the FE models with cemented femoral prostheses: (a) ABG-cemented and (b) Versys.

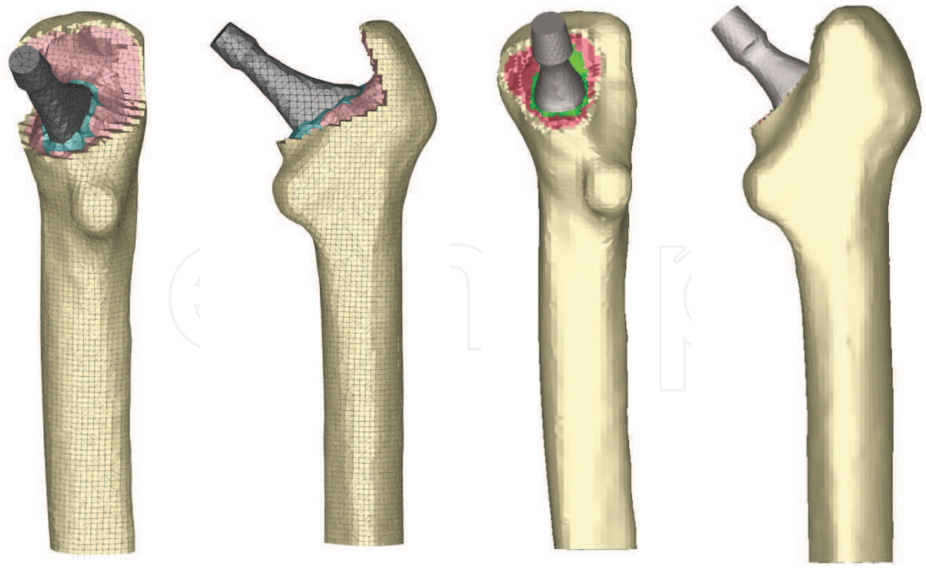

(a) (b)

Fig. 17. FE model with cemented femoral prostheses: (a) ABG-cemented and (b) Versys.

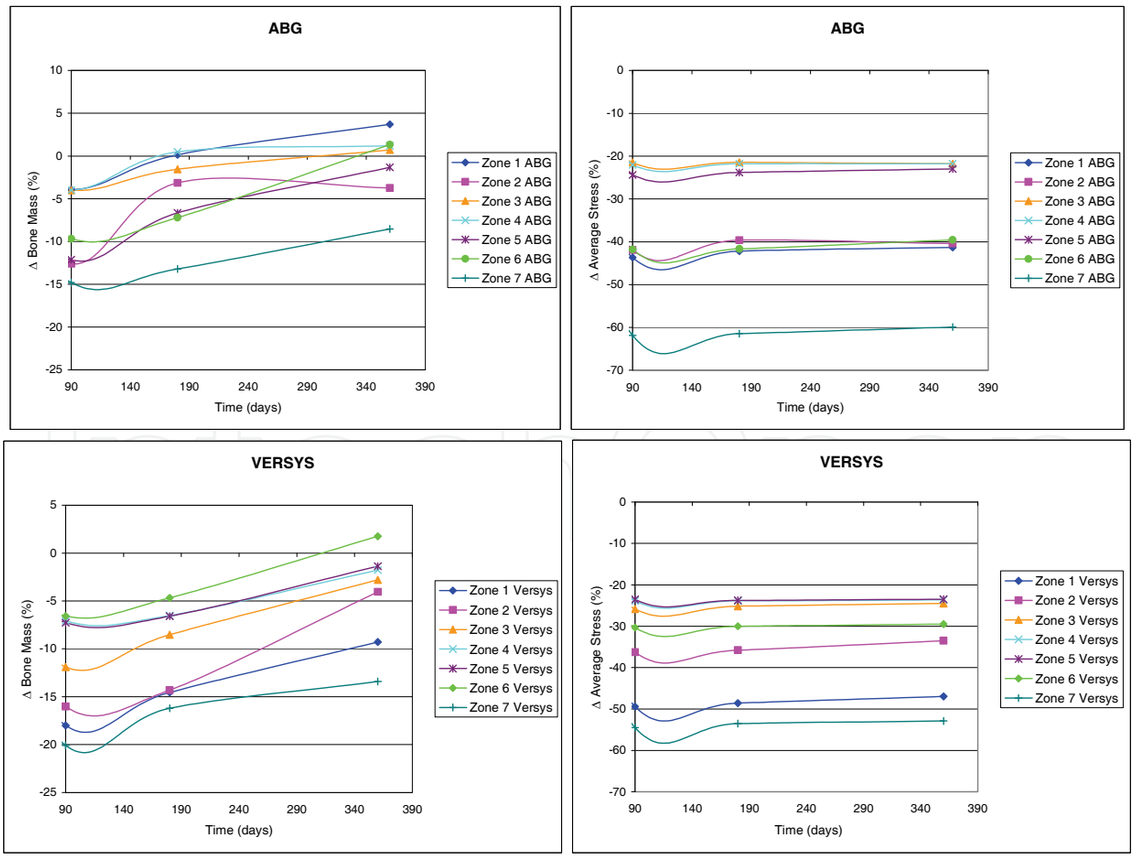

Fig. 18. BMD and average von Mises stress evolution

Both models were meshed with tetrahedral solid elements linear type, with a total of 74192 elements in the model for ABG-cemented prosthesis (33504 items cortical bone, cancellous bone 17859, 6111 for the ABG stem-cement, cement 13788 and 2930 for diaphyseal plug), and 274651 in the model for prosthetic Versys (119151 items of cortical bone, cancellous bone 84836, 22665 for the Versys stem, 44661 for the cement and 3338 in diaphyseal plug). In Fig. 17 are shown both models for cemented stems.
Calculation was performed using the program Abaqus 6.7. Both prostheses have been simulated with the same mechanical properties, thus, the result shows the influence of stem geometry on the biomechanical behavior. Fig. 18 shows the variation (%) of bone mass and average von Mises stress (%) in each of the Gruen zones for each of the models of cemented prostheses, with reference to the preoperative time. It can be seen that for both stems, the maximum decrease in bone mass occurred in Zone 7. This decrease in bone mass is greater in the Versys model than in the ABG stem
Prior to the development of our FE models several long-term studies of bone remodeling after the implantation of two different cementless stems, ABG I and ABG II, were performed (Panisello et al., 2006; Panisello et al., 2009a; Panisello et al., 2009b). These studies were performed using DEXA, a technique that allows an accurate assessment of bone density losses in the different Gruen zones (Fig. 19). We take as a reference to explore this evolution, the postoperative value obtained in control measurements and those obtained from contralateral healthy hip. New measurements were made at 6 months, one year and 5 years after surgery. The ABG II stem is an evolution of the ABG I, which has been modified both in its alloy and design. The second generation prosthesis ABG-II is manufactured with a different titanium alloy from that used in the ABG-I. The prosthetic ABG-I stem is made with a Wrought Titanium alloy (Ti 6Al-4V) of which elasticity modulus is 110 GPa. Meanwhile, the TMZF alloy, which is used on the ABG-II stem, has a Young's modulus of 74-85 GPa, according to the manufacturer information, using a mean value of 79.5 GPa in the different analyses. On the other hand, the ABG II stem has a new design with less proximal and distal diameter, less length and the shoulder of stem has been redesign to improve osteointegration in the metaphyseal area.

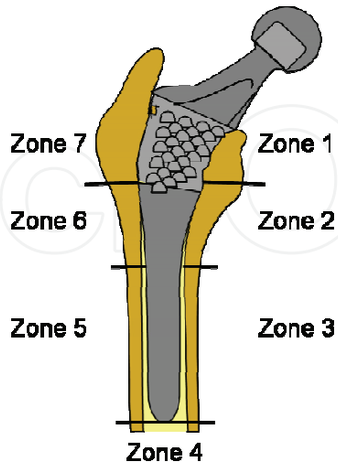

Fig. 19. Gruen zones

In our DEXA studies, directed to know the loss of bone mass in the different zones of Gruen caused by the stress-shielding, we found that ABG II model produces less proximal bone

atrophy in post-operative measurements, for similar follow-up periods. In the model ABG II, we keep finding in studies with DEXA a proximal bone atrophy, mainly in zones 1 and 7 of Gruen, but with an improvement of 8.7% in the values obtained in ABG I series. We can infer that improvements in the design of the stem, with a narrower diameter in the metaphyseal area, improve the load transfer to the femur and therefore minimizes the stress-shielding phenomenon, resulting in a lower proximal bone atrophy, because this area receive higher mechanical stimuli. These studies for determination of bone mass in Gruen zones, and the comparative study of their postoperative evolution during 5 years have allowed us to draw a number of conclusions: A) Bone remodeling, after implantation of a femoral stem, is finished one year after surgery B) Variations in bone mass, after the first year, are not significant.

The importance of these studies is that objective data from a study with a series of patients, allow us to confirm the existence of stress-shielding phenomenon, and quantify exactly the proximal bone atrophy that occurs. At the same time they have allowed us to confirm that the improvements in the ABG stem design, mean in practice better load transfer and less stres-shielding phenomenon when using the ABG II stem.

DEXA studies have been basic to validate our FE models, because we have handled real values of patients' bone density, which allowed us to measure mechanical properties of real bone in different stages. Through computer simulation with our model, we have confirmed the decrease of mechanical stimulus in femoral metaphyseal areas, having a higher stimulus in ABG II type stem, which corresponds exactly with the data obtained in studies with DEXA achieved in patients operated with both models stems.

In the case of cemented stems, densitometric studies were performed with two different types of stem: one straight (Versys, manufactured in a cobalt-chromium alloy) and other anatomical (ABG , manufactured in forged Vitallium patented by Stryker Howmedica). It was carried on the same methodology used in the cemented stems series, but postoperative follow-up was only one year long. Densitometric studies previously made with cementless stems allow us to affirm that bone remodeling is done in the first postoperative year, a view shared by most of the authors. So, we accept that bone mineral density values obtained one year after surgery can be considered as definitive. As in cementless models, densitometric values have been used for comparison with those obtained in the FE simulation models. Our studies confirmed that the greatest loss of bone density affects the area 7 of Gruen (Joven, 2007), which means that stress-shielding and atrophy of metaphyseal bone also occurs in cemented prostheses. This phenomenon is less severe than in non-cemented stems, therefore we can conclude that the load transfer is better with cemented stems than with cementless stems. The findings of proximal bone atrophy, mainly in the area 7, agree with those published by other authors (Arabmotlagh et al., 2006; Dan et al., 2006). We have also found differences in the rates of decrease in bone density in the area 7 of Gruen, wich were slightly lower in the anatomical ABG stem than in the Versys straight stem. This also indicates that the prosthesis design has influence in the remodeling process, and that mechanical stimuli are different and related to the design.

4. Application to the lumbar spine

The spine is a complex anatomical structure that has triplanar movements, maintains the erect posture of the individual and supports a significant load. In its central part forms the

spinal canal to contain the nervous structures, therefore has to combine the flexibility to perform movements and to maintain stability and protect nervous structures. The spine changes its mechanical properties depending on the loads, therefore behaves as a viscoelastic structure (Yaszemski at al., 2002). For these special features the study of its biomechanics, in its three areas, is a very complex matter. And it is very difficult to reproduce it for in vivo or in vitro studies. Of the whole of spine, lumbar spine has been widely studied, showing in many papers, a large variability of results.

Biomechanics of the lumbar spine has been studied in cadaveric specimens (Panjabi et al., 1994). But lack of flexibility makes difficult to reproduce the range of motion presented by living persons. In vivo studies has been made by various methods (radiographic, CTA, IMR, TV and computer, electrogoniometer, inclinometer, etc.). The results are extremely variable, even for the same person throughout the day (Ensink et al., 1996) and also have different values on account of age and existing pathology (Sillivan et al., 1994). Animal spines have also been used for these biomechanical studies, despite major differences with the human lumbar spine (Kettler et al., 2007).

Because of the difficulties to research with living persons, their variability with mixed results published, the problems arisen with in vitro studies and differences between human and animal column, we have developed simulation models, using finite elements (FE). This model allows to research on lumbar spine, in physiological conditions, to simulate different load conditions and study the impact on biomechanics. We can also simulate the disc degeneration, to a greater or lesser degree, and study the impact on adjacent elements to degenerated disc. Finally, the model may be useful to test different fixation systems, as a pedicular screw, a interbody device or rigid fixations compared with the dynamics.

By using the methodology described in §1, it is possible to obtain the geometrical model corresponding to the S1-L5 functional unit (Fig. 20).

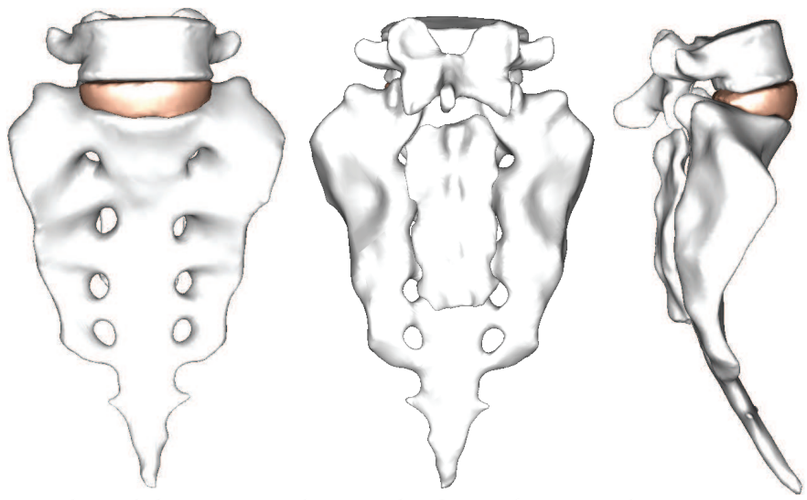

Fig. 20. Geometrical model corresponding to the S1-L5 functional unit

The mesh of the vertebrae is made by means of tetrahedrons with linear approximation in the I-deas program (I-deas, 2007) with a size thin enough to allow a smooth transition from the zone of exterior cortical bone to the zone of interior cancellous bone; this transition was obtained by means of statistical averages from CTs of vertebrae in healthy individuals. Disc

meshes are essential for a correct reproduction of the biomechanical behaviour of the functional unit analysed. In order to do this, each disc is divided into nucleus pulposus and annulus fibrosus with commonly accepted dimensions (White & Panjabi, 1990). Each part is meshed separately so that mesh sizes should match each other and with the vertebrae, getting the complete FE model (Fig. 21).

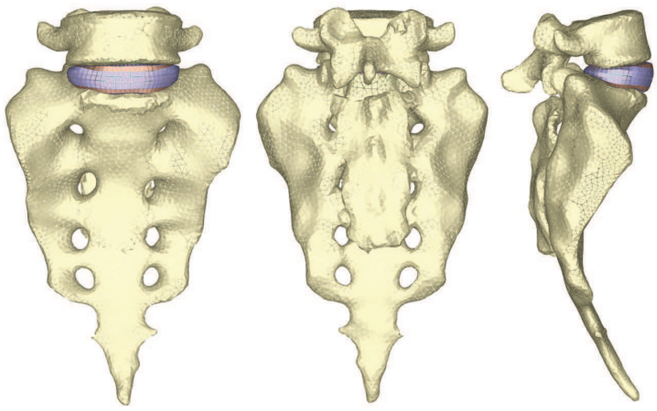

Fig. 21. FE model corresponding to the S1-L5 functional unit

Concerning material properties, those of bone were taken from literature. About discs, nucleus pulposus behaves like a non-compressible fluid, which upon being compressed expands towards the exterior tractioning the fibers of the annulus. Fibers of the annulus show a hyperelastic behaviour, but only in tension. The correct interaction between the different elements (vertebrae, discs and ligaments) is essential. Conditions of union between the vertebral body and the intervertebral disc have been established, as it is the most representative of the real anatomy. Finally, contact conditions have been established between the different apophysis which provides a global stability. In order to verify the effectiveness of the fixation, flexion-extension movement has been analyzed as the most representative (Fig. 22). As boundary conditions displacements in the alas of sacrum have been prevented.

Fig. 22. Flexion-extension movement of the S1-L5 functional unit

Muscle and ligament forces are adjusted to the apropriate values to obtain the required movement ranges. So, the deformed shapes shown in Fig. 23 are achieved. Calculation and post-processing are carried out using the Abaqus program (Abaqus, 2009).

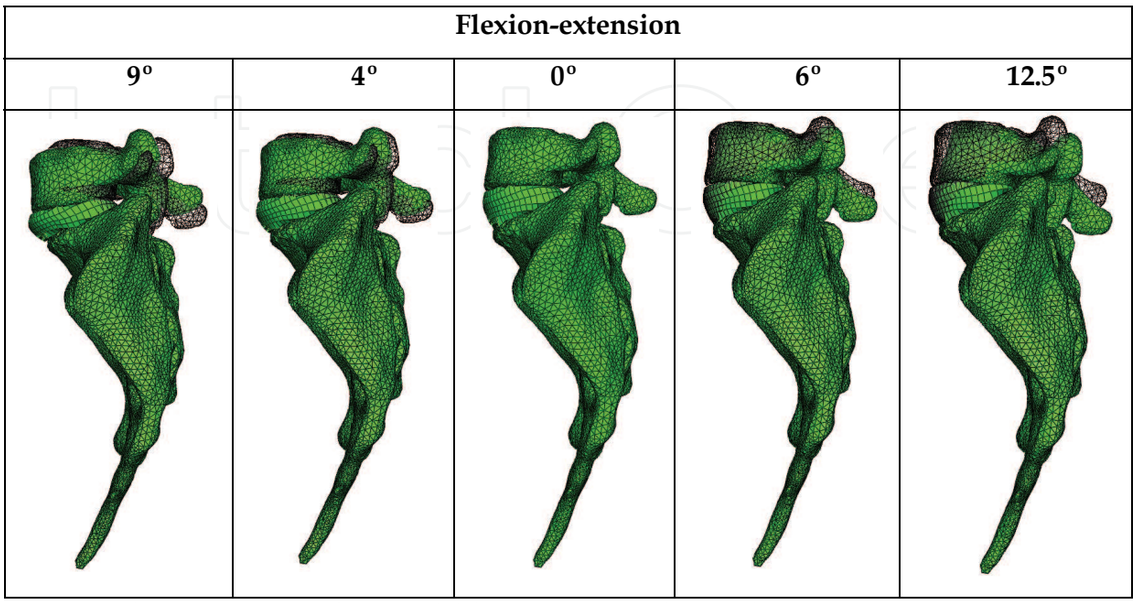

Fig. 23. Deformed shapes of the S1-L5 functional unit for the flexion-extension movement

Once the healthy model has been adjusted and validated, it is possible to simulate new conditions corresponding to different levels of discal degeneration. So, after decreasing the mechanical properties of annulus and fibers in the disc, according with the mechanical damage theory, we can measure the changes produced in the different movements.
The next step is the study of several types of fixations (rigid and dynamic). Changes induced by surgery must be reproduced in the FE model. To that effect, the holes for the pedicular screws must be generated by removing the elements intersectected by the screws, and reseting the mesh along the new interfaces. In the same way, pedicular wings must be trimmed to allow the introduction of the screws. With the screws in place, the struts are implemented to obtain the final models (Figs. 24 & 25).

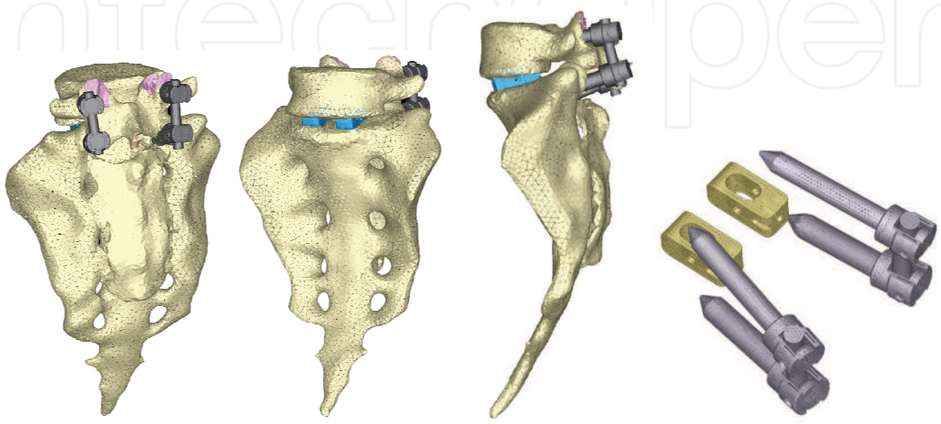

Fig. 24. FE model corresponding to the S1-L5 functional unit with rigid fixation

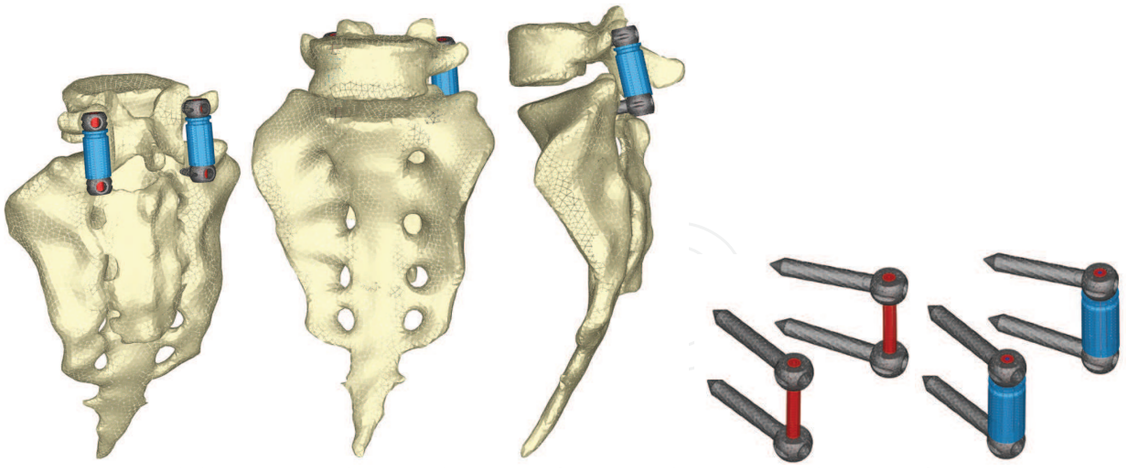

Fig. 25. FE model corresponding to the S1-L5 functional unit with dynamic fixation

From those new models the study of the flexion-extension movement can be reproduced in the new conditions, verifying the changes produces as consequence of the fixations. The results allow comparing the performance of the different models, and moreover it is possible to analyse the changes in the local stress distribution around the screws detecting points of possible future pathologies due to the alterations produces by the presence of the fixations. So, in Figs. 26 and 27 the von Mises stress distribution, both in the healthy and in the implanted models, are shown. Comparing both Figs., a high stress concentration around the screw root is observed, increasing the maximum value till 400% with respect to the healthy model.

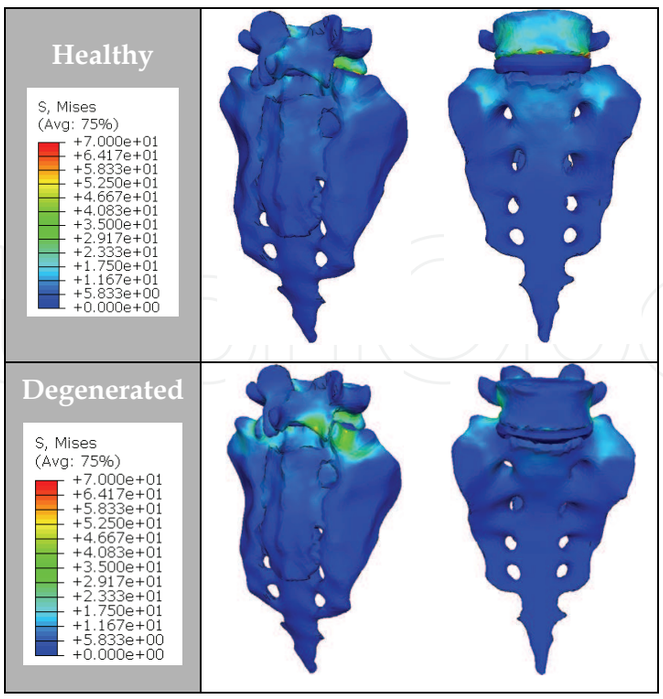

Fig. 26. Von Mises stresses for the healthy and degenerated models

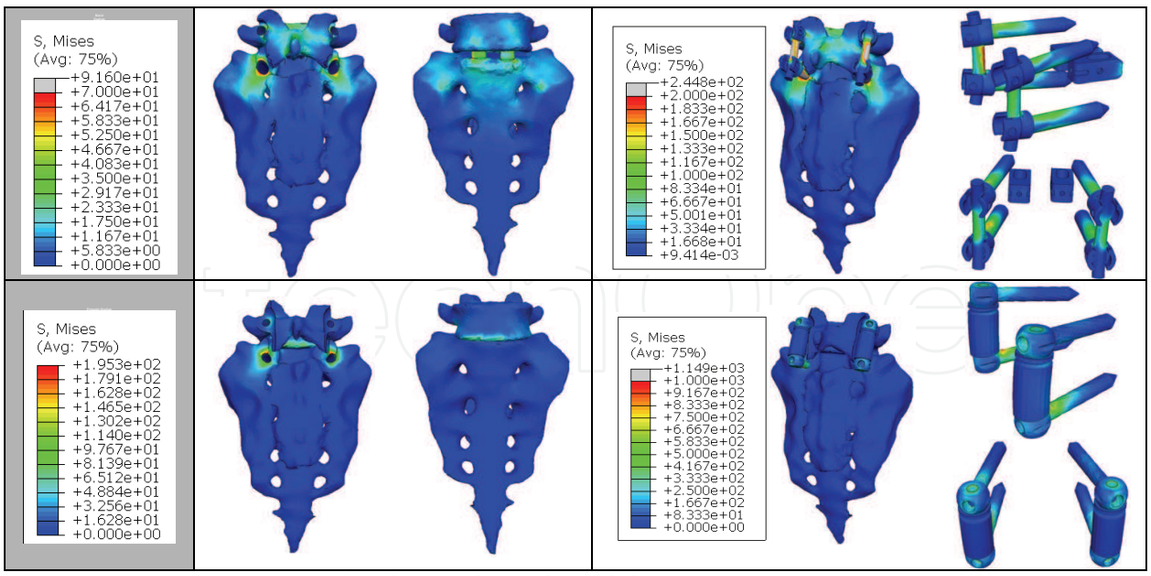

Fig. 27. Von Mises stresses for the implanted models

Future research concerns the development of the complete lumbar spine model, from S1 to L1, including ligaments and cartilages, in order to get a better approximation to the real biomechanical behaviour.

5. Application to splints for hand therapy

In the pathology of the hand is often the existence of joint stiffness, usually post-traumatic, causing vicious positions and loss of mobility of the joints. Also rheumatic disease that affects the joints of the hand, can cause deformity and changes in normal joint alignment. The worst situation occurs when these alterations produce one flexion stiffness of the joints

In the treatment of articular rigidities the usual therapy consists of the application of splints, which utility is guaranteed by different clinic studies that demonstrated its efficacy in most of the pathologies (Prosser, 1996).

The mission of the orthopedics splints is relieve the strength they have or to keep a constant tension, in a determinate mode in the joints and stimulate, that way, the hisitic changes which allow the stretching of the capsule and joint structures until the deformity is corrected. Among all the different pathologies affecting the hand , due to traumas or sickness, one of the more frequent is the contracture by flexion of the proximal interphalangeal joint (AIP). This joint and its mobility are one of the most important factors in the hand functionality.

The use of materials with shape memory and superelastic behaviour like NiTi for the manufacture of orthopedic splints is a possibility with great expectations for the future. The experience of the authors in the design of other devices based on the NiTi alloy (Puértolas et al., 2002; Lahoz et al., 2002; Domingo et al., 2005; Domingo et al., 2006), makes it possible to carry out the proposed design of a finger splint for the treatment of the contracture in flexion of the PIP joint. About the material, NiTi is an equiatomic alloy of nickel and titanium (commercially known as Nitinol), discovered in the U.S. Naval Ordenance Laboratory (Buehler & Wiley, 1965). It belongs to a group of materials with shape memory (SMA). Basically, these alloys have the

attribute of being able to recover a previously defined form when the material is subjected to an adequate thermal treatment; associated to this behaviour, the material has a super elasticity which lends to the property of withstanding large elastical deformations with relatively low tensions. This property is due to the change of phase which the material undergoes when it is subjected to tension (Auricchio & Petrini, 2002).

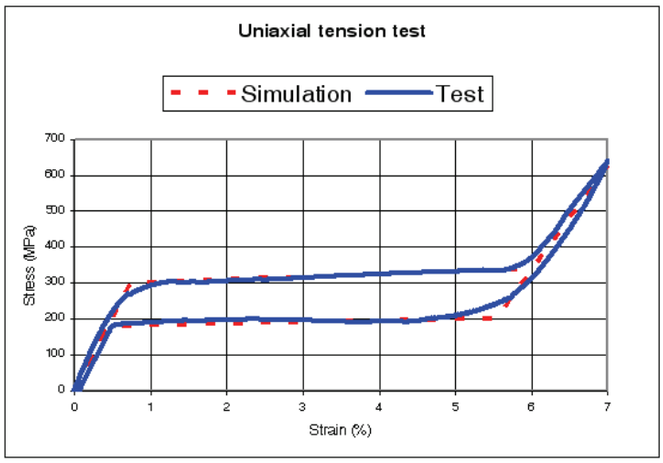

Fig. 28. Stress-strain curve for loading and unloading process corresponding to the NiTi alloy at 22º C

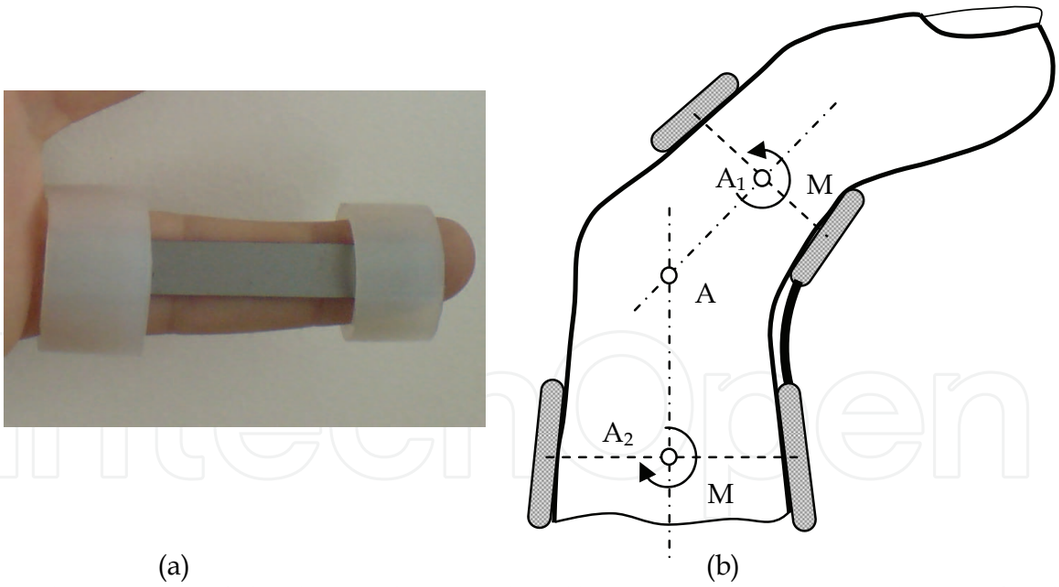

(a) (b)

Fig. 29. a) Prototype of the designed NiTi splint; b) Force transmission mechanism for the designed splint

The first step corresponds to characterization of the basic behaviour of the material, because the mechanical properties of NiTi are very sensitive to little changes in the alloy composition. For this reason, it is necessary to carry out tension-compression uniaxial standard test in the overall range of strains, obtaining the whole behaviour curve both for

loading and unloading processes. With this purpose, a universal machine INSTRON 5565 was used to testing standard test specimens obtained from shells 1 mm width corresponding to a reference alloy (50.8% Ni, 49.2% Ti) supplied by the company Memory Metalle GBMH. This alloy exhibits a superelastic behaviour at environment temperature. In every test a complete loading-unloading cycle with displacement control is reached till a maximum strain of 7% at 22º C. In Fig. 28 the tension curve is shown, evaluating from that the different mechanical parameters: elastic moduli for martensite and austenite phases (E_A, E_M), respectively, phase transition stresses (σ_s^{Am}, σ_f^{AM}, σ_s^{MA}, σ_f^{MA}) and maximum strain (ε_L). The proposed design uses a thin plate of NiTi, which is fixed onto the finger by means of rings, which are responsible for transmitting the recovering force (Fig. 29). The mechanism provides a practically unidimensional bending performance, such that the device presents a mechanical response close to the intrinsic material behaviour. This means that the moment-angle curve of the splint has a similar shape to the material tension-deformation curve.

Parameter	Description	Value
E_A	Austenite Young Modulus	52650 MPa
ν_A	Austenite Poisson Ratio	0.33
E_M	Martensite Young Modulus	38250 MPa
ν_M	Martensite Poisson Ratio	0.33
ε_L	Maximum Transformation Strain	6%
σ_s^{AM}	Transformation Activation Stress (A→M)	300 MPa
σ_c^{AM}	Transformation Completion Stress (A→M)	340 MPa
σ_s^{MA}	Transformation Activation Stress (M→A)	200 MPa
σ_c^{MA}	Transformation Completion Stress (M→A)	180 MPa
T_0	Reference Temperature	22 ºC
C^{AM}	$\frac{\partial \sigma_{s,c}^{AM}}{\partial T}$	6.7 MPa/ºC
C^{MA}	$\frac{\partial \sigma_{s,c}^{MA}}{\partial T}$	6.7 MPa/ºC

Table 2. Material properties (NiTi)

The action of the splints is directly related to the rigidity, and in the proposed design the rigidity is directly related to the width, the thickness and the length, although all of these geometric factors work in an uneven way. An increase in width supposes a linear growth in the recovering force and a better finger support. However, the most important factor used to control the force exerted by the splint is the plate thickness. The device is very sensitive to thickness change, presenting a cubic rate influence. Hence, the greater the thickness, the greater the effect of straightening and the smaller the risk of breakage although it is more

difficult to bend the splint and fit it in the volar zone of the injured finger. On the contrary, if the thickness is reduced so is the straightening effect and the risk of breakage increases, although it is easier to bend the splint and fit it on the finger.
To obtain a design which transmits a force adequate for the recovery of the original position of the finger, a finite elements simulation for a plate of these dimensions, 80x10x1 mm, is carried out. For the behaviour of the material a proprietary developed user subroutine is used, based on Auricchio`s models (Auricchio & Petrini, 2002), in the Abaqus program (Abaqus, 2009). Previously, an adjustment of parameters from the results of the tensile test is carried out (Fig. 28). The different parameters used in the simulation are gathered in Table 2. As for the boundary conditions, initially a displacement of 1 mm in the centre of the plate is applied to later apply the eccentric compression until reaching the maximum curvature, moment in which the load is removed and a free restoration is produced.
Fig. 30. shows the von Mises stress maps in both faces (top and bottom) of the shell for different curvatures in the whole range of deformation, while Fig. 31 shows the martensite fraction maps for the same leves of deformation as Fig. 30.

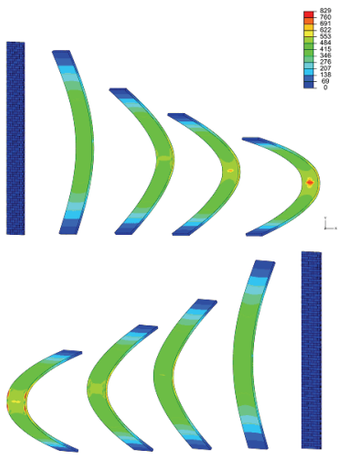

Fig. 30. Von Mises stress maps

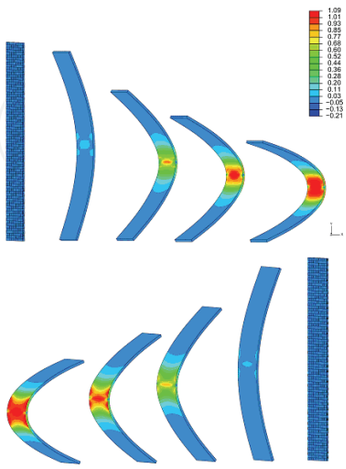

Fig. 31. Martensite fraction maps

Once the model was adjusted, a parametric study was carried out with different values of length, width and thickness for the plate. Figs. 32 and 33 show the Recovering Force-Angle curves for the different lengths and widths of the plate, with a fixed thickness of 1mm, and the Recovering Force-Angle curves for different lengths and thicknesses of the plate, with a fixed width of 6mm. A practically constant recovering force value can be observed over a wide range of angles that vary between 30º and 150º. This makes it possible to define a characteristic value of recovering force which is ascribed to an angle flexion of 80º. The same occurs in all of the cases analysed.

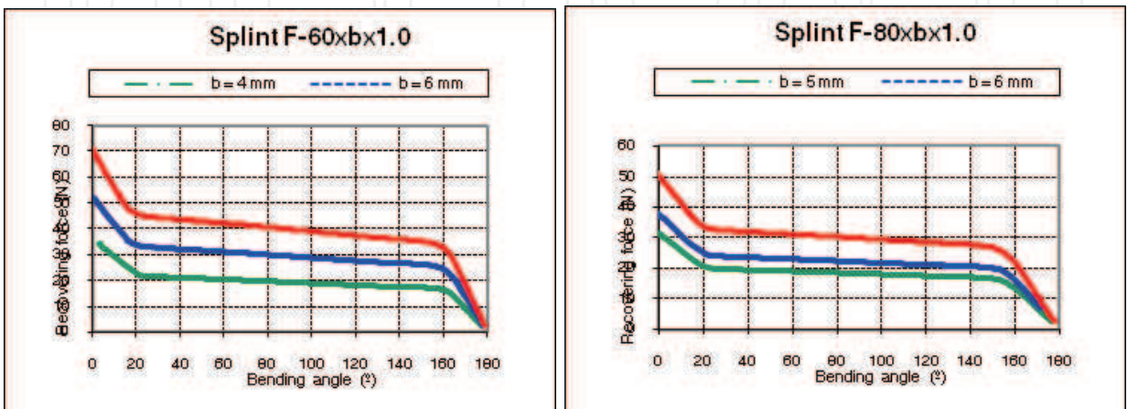

(a) (b)

Fig. 32. Recovering force-Angle curves: (a) Length 60.0 mm, width variable, thickness 1.0 mm; (b) Length 80.0 mm, width variable, thickness 1.0 mm

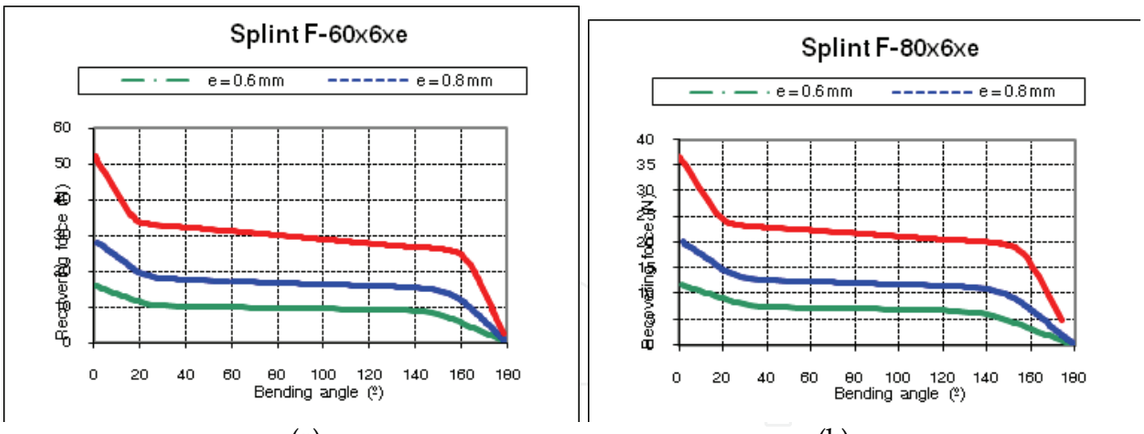

(a) (b)

Fig. 33. Recovering force-Angle curves (a) Length 60.0 mm, width 6.0 mm, thickness variable; (b) Length 80.0 mm, width 6.0 mm, thickness variable

In order to design a NiTi prosthesis with a recovering force equivalent to the usual in commercial orthosis, it is necessary to adjust the rigidity to bending to the value of this. A parametric simulation has been carried out, covering a range of forces from 5 to 30 N, with lengths and widths capable of adapting to fingers of different sizes. One main advantage of the proposed designs is that they achieve a practically constant recovering force in a range

of angles from 20º to 150º. This makes possible a therapeutic device that practically covers the total recovery of the PIP joint. In Fig. 34, comparative values of simulation versus experimental results are presented.

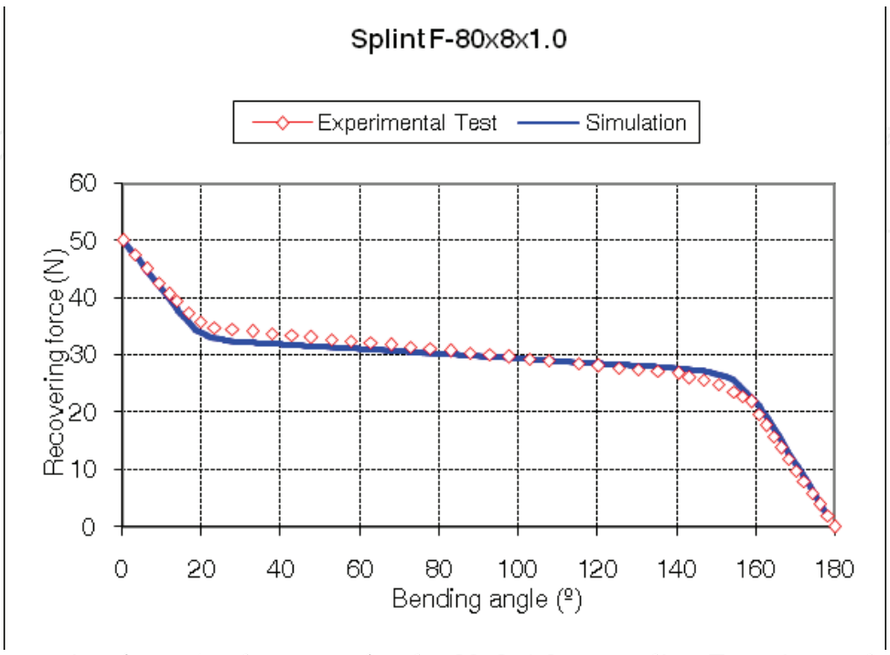

Fig. 34. Recovering force-Angle curves for the 80x8x1.0 mm splint. Experimental test versus simulation

Apart from the properties of NiTi, the biomechanical behaviour of the proposed splint compared to the commercial ones analysed is totally different due to its design. Hence, the mechanism to transmit forces onto the finger in the Bort class of splints (and in the majority of those that exist on the market) is based on equilibrium in a simple bending situation, with action (F_1, F_2) and reaction (F_3) in the different parts of the splint (Fig. 35). On the contrary, in the developed prototype the transmission mechanism is based on equilibrium in pure bending, transmitting both torques on the fixation rings (Fig. 29), through the local equilibrium of forces in the fixation rings.

The common bending mechanism has two important drawbacks: firstly, for a linear behaviour spring the ratio between recovering force and angle is constant in its whole length. Hence, as recovery is produced the torque transmitted on the joint decreases significantly, even though the distance from the point where the force is applied F_1 on the joint, point A in Fig. 35 becomes progressively larger. Its increase does not compensate the loss of force, for which it is necessary to change the splint for another with a different force calibration. Moreover, the forces involved in the equilibrium have components that can generate compression or traction on the joint itself, possibly increasing the damage to the joint.

However, in the mechanism of pure bending as it is directly transmitting torques, the effect on the joint is always the same in all of the recovering range. In addition forces are not generated on joints; the forces are generated at local level on the fixation rings to give rise to the torques transmitted, acting on zones that are away from the joint and without damaging

effects. Thus the recovering moment is constant in all of the length A_1-A-A_2 (Fig. 29b), without producing undesired effects on the joint. Given that the splint reproduces in the graph moment-angle the basic behaviour of NiTi in the tensile test, the recovering moment is practically constant in the all of the range where the splint works. Then the whole treatment is possible with only one splint, and without the need of progressive replacements as the joint recovers.

No other splint available on the market offers this property since all of them are based on materials and mechanisms in which global result is that of a cuasi-linear behaviour. This makes it impossible to obtain the curves with a practically null slope in the recovery stage like the one presented here.

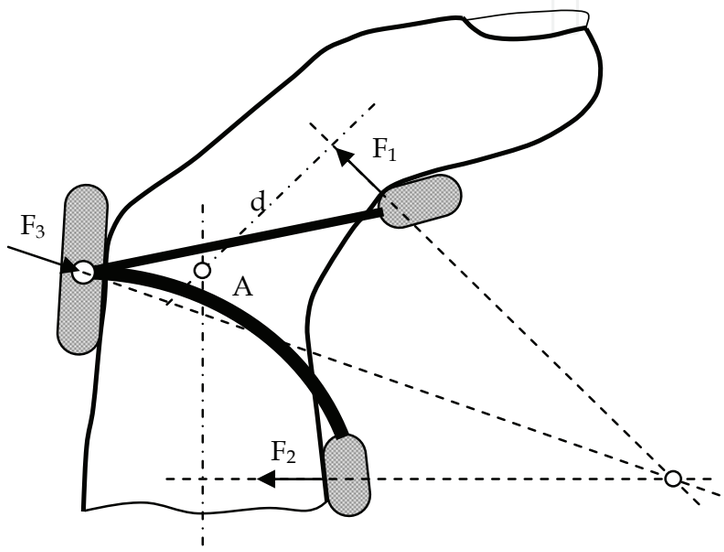

Fig. 35. Force transmission mechanism for Bort type splints.

Another talking point is the optimum time for the use of straightening splints, which Flower defined as TERT (Total End Range Time) (Flower & LaStayo, 1994), having checked that the longer it is worn daily the better the results (Flower & LaStayo, 1994; Flower, 2002). However, Flower himself concludes that in addition to the time of use, the force application parameters are fundamental in attaining a good correction of the deformity (Flower, 2002). Due to its comfort the proposed design makes it possible to wear permanently. On the other hand, permanent action dynamic orthosis, regularly used in orthopaedics for the PIP joint, are difficult to fit, above all at the level of the proximal phalange despite the therapist being able to choose the size.

On the contrary, the designed splint in this work improves the initial adjustment and make it easier to use for both the patient and the specialist, with no difficulties in its fitting. The proposed design also avoids the harmful effect of pressure on the back of the joint (Li, 1999) which is produced in the usual static and dynamic systems. The advantages offered against the most frequently used commercial models can be summarised as:

- Better control of the recovering force.
- Maintaining the splint over long periods of time without replacement, since its effect remains unalterable over a wide period of recuperation.
- Ease of use for both the patient and specialist.

- Ease of producing custom made designs for each patient.
- Significant economic saving in the treatment.

For all of the above mentioned, the proposed design is highly competitive compared to those used presently. The future research concerns the design of alternative geometries and the improvement of the fixation system.

6. References

ABAQUS. (2009). Web site, http://www.simulia.com/.

Arabmotlagh, M.; Sabljic, R. & Rittmeister, M. (2006). Changes of the biochemical markers of bone turnover and periprosthetic bone remodelling after cemented arthroplasty. *J Arthroplasty*, 21,1, 129-34. ISSN: 0883-5403

Auricchio, F. & Petrini, L. (2002). Improvements and algorithmical considerations on a recent three-dimensional model describing stress-induced solid phase transformations. *Int J Numer Meth Eng*, 55, 1255-1284. ISSN: 0029-5981

Bathe, K.J. (1982). *Finite element procedures in engineering analysis*, Prentice-Hall, New Jersey. ISBN-10: 0133173054

Buckwalter, J.A.; Glimcher, M.J.; Cooper, R.R. & Recker, R. (1995). Bone biology, *J Bone Joint Surg,* 77A , 1276-1289. ISSN: 0021-9355

Buehler, W.J. & Wiley, R.L. (1965). *Nickel-base alloys,* U.S. Patent 3.174.851.

Dan, D.; Germann, D.; Burki, H.; Hausner, P.; Kappeler, U.; Meyer, R.P.; Klaghofer, R. & Stoll, T. (2006). Bone loss alter total hip arthroplasty. *Rheumatol Int*, 26, 9, 792-8. ISSN: 0172-8172

Denozière, G. & Ku, D.N. (2006). Biomechanical comparison between fusion of two vertebrae and implantation of an artificial intervertebral disc. *J Biomechanics*, 39,766-755. ISSN: 0021-9290

Domingo, S.; Puértolas, S.; Gracia, L. & Puértolas, J.A. (2006). Mechanical comparative analysis of stents for colorectal obstruction. *Minim Invasiv Ther,* 15, 6, 331-338. ISSN: 1364-5706

Domingo, S.; Puértolas, S.; Gracia, L.; Mainar, M.; Usón, J. & Puértolas, J.A. (2005). Design, manufacture and evaluation of a NiTi stent for colon obstruction. *Bio-Med Mater Eng*, 15, 5, 357-365. ISSN: 0959-2989

Ensink, F.B.; Saur, P.M.; Frese, K.; Seeger, D. & Hildebrandt, J. (1996). Lumbar range of motion: influence of time of day and individual factors on measurements. *Spine*, 21, 11, 1339-43. ISSN: 0362-2436

Evans, F.G. (1973). *Mechanical properties of bone*, Evans F.G. (Ed), Ed. Springfield, Illinois.

Flower KR. (2002). A proposed decision hierarchy for splinting the stiff joint, with an emphasis on force application parameters. *J Hand Ther,* 15, 158-162. ISSN: 0894-1130

Flower, K.R. & LaStayo, P. (1994). Effect of total end range time on improving passive range of motion. *J Hand Ther*, 7, 150-157. ISSN: 0894-1130

Gibbons, C.E.R.; Davies, A.J.; Amis, A.A.; Olearnik, H.; Parker, B.C. & Scott, J.E. (2001). Periprosthetic bone mineral density changes with femoral components of different design philosophy. *In Orthop*, 25, 89-92. ISSN: 0341-2695

Glassman, A.H.; Crowninshield, R.D.; Schenck, R. & Herberts, P. (2001). A low stiffness composite biologically fixed prostheses. *Clin. Orthop*, 393, 128-136. ISSN: 0009-921X

Guan, Y.; Yoganandan N.; Zhang, J.; Pintar, F.A.; Cusick, J.F.; Wolfla, Ch. E. & Maiman, D.J. (2006). Validation of a clinical finite element model of the human lumbosacral spine. *Med Bio Eng Comput*, 44, 633-641. ISSN: 0140-0118

Herrera, A.; Panisello, J.J.; Ibarz, E.; Cegoñino, J.; Puertotas, J.A. & Gracia, L. (2009). Comparison between DEXA and Finite Element studies in the long term bone remodelling o an anatomical femoral stem. *J Biomech Eng*, 31, 4, 1004-13. ISSN: 0148-0731

Herrera, A; Panisello, J.J.; Ibarz, E.; Cegoñino, J.; Puertotas, J.A. & Gracia, L. (2007). Long term study of bone remodelling after femoral stem: a comparison between Dexa and finite element simulation. *J Biomechanics*, 40, 16, 3615-25. ISSN: 0021-9290

Hughes, T.J.R. (1987). *The finite element method*, Prentice-Hall, New Jersey. ISBN-10 013317025X

Huiskes, R.; Weinans, H. & Dalstra, M. (1989). Adaptative bone remodeling and biomechanical design considerations for noncemented total hip arthroplasty. *Orthopedics*, 12, 1255-1267. ISSN: 0147-7447

I-DEAS. (2007). Web site, http://www.ugs.com/.

Imbert, F.J. (1979). *Analyse des structures par élément finis*, Cepadues Edit, Toulouse. ISBN: 2854280512

Joven, E. (2007). *Densitometry study of bone remodeling in cemented hip arthroplasty with stem straight and anatomical*. Doctoral Degree Disertation, University of Zaragoza.

Kerner, J.; Huiskes, R.; van Lenthe, G.H.; Weinans, H.; van Rietbergen, B.; Engh, C.A. & Amis, A.A. (1999). Correlation between pre-operative periposthetic bone density and post-operative bone loss in THA can be explained by strain-adaptative remodelling. *J Biomechanics*, 32, 695-703. ISSN: 0021-9290

Kettler, A.; Liakos, L.; Haegele, B. & Wilke, H.J. (2007). Are the spines of calf, pig and sheep suitable models for pre-clinical implant tests?. *Eur Spine J*, 16, 12, 2186-92. ISSN: 0940-6719

Lahoz, R.; Gracia, L. & Puértolas, J.A. (2002). Training of the two-way shape memory effect by bending in NiTi alloys. *J Eng Mater-T*, 124, 4, 397-401. ISSN: 0094-4289

Li, C. (1999). Force analysis of the Belly Gutter and Capener splints. *J Hand Ther*, 12, 337-343. ISSN: 0894-1130

Li, M.G.; Rohrl, S.M.; Wood, D.J. & Nivbrant, B. (2007). Periprosthetic Changes in Bone Mineral Density in 5 Stem Designs 5 Years After Cemented Total Hip Arthroplasty. No Relation to Stem Migration. *J Arthroplasty*, 22, 5, 698-91. ISSN: 0883-5403

Little, J.P.; Adam, C.J.; Evans, J.H.; Pettet, G.J. & Pearcy, M. J. (2007). Nonlinear finite element analysis of anular lesions in the L4/5 intervertebral disc. *J Biomechanics*, 40, 2744-2751. ISSN: 0021-9290

Marklof, K.L.; Amstutz, H.C. & Hirschowitz, D.L. (1980). The effect of calcar contact on femoral component micromovement.A mechanical study. *J Bone Joint Surg*, 62A, 1315-1323. ISSN: 0021-9355

McAuley, J., Sychterz, Ch. & Ench, C.A. (2000). Influence of porous coating level on proximal femoral remodeling. *Clin Orthop Relat R*, 371, 146-153. ISSN: 0009-921X

MIMICS. (2010). Web site, www.materialise.com.

Panisello, J.J.; Herrero, L.; Herrera, A.; Canales, V.; Martínez, A.A. & Cuenca, J. (2006). Bone remodelling after total hip arthroplasty using an uncemented anatomic femoral stem: a three-year prospective study using bone densitometry. *J Orthop Surg*, 14, 122-125. ISSN: 1022-5536

Panisello, J.J.; Canales, V.; Herrero, L.; Herrera, A.; Mateo, J. & Caballero, M.J. (2009). Changes in periprosthetic bone remodelling alter redesigning an anatomic cementless stem. *Inter Orthop*, 33, 2, 373-380. ISSN: 0341-2695

Panisello, J.J.; Herrero, L.; Canales, V.; Herrera, A.; Martínez, A.A. & Mateo, J. (2009). Long-term remodelling in proximal femur around a hydroxiapatite-coated anatomic stem. Ten years densitometric follow-up. *J Arthroplasty*, 24, 1, 56-64. ISSN: 0883-5403

Panjabi, M.M.; Oxland, T.R.; Yamamoto, I. & Crisco, J.J. (1994). Mechanical behavior of the human lumbar and lumbosacral spine as shown by three-dimensional load-displacement curves. *J Bone Joint Surg Am*, 76, 3, 413-24. . ISSN: 0021-9355

Prosser, R. (1996). Splinting in the management of proximal interphalangeal joint flexion contracture. *J Hand Ther*, 9, 378-386. ISSN: 0894-1130

Puértolas, J.A.; Pérez-García, J.M.; Juan, E. & Ríos, R. (2002). Design of a suture anchor based on the superelasticity of the Ni-Ti alloy. *Biomed Mater Eng*, 12, 3, 283-289. ISSN: 0959-2989

Radin, E.L. (1980). Bimechanics of the Human hip. *Clin Orthop Relat R,* 152, 28-34. ISSN: 0009-921X

Ramaniraka, N.A.; Rakotomanana, L.R. & Leyvraz, P.F. (2000). The fixation of the cemented femoral component .Effects of stem stiffness, cement thickness and roughness of the cement-bone surface . *J Bone Joint Surg*, 82Br, 297-303. ISSN: 0301-620X

Rubash, H.E.; Sinha, R.K.; Shanbhag, A.S. & Kim, S.Y. (1998). Pathogenesis of bone loss after total hip arthroplasty. *Orthop Clin N Am*, 29(2), 173-186. ISSN: 0030-5898.

Sullivan, M.S.; Dickinson, C.E. & Troup, J.D. (1994). The influence of age and gender on lumbar spine sagittal plane range of motion. A study of 1126 healthy subjects. *Spine*, 19, 6, 682-6. ISSN: 0362-2436

Sumner, D.R. & Galante, J.O. (1992). Determinants of stress shielding :desing versus materials versus interface. *Clin Orthop Relat R*, 274, 202-12. ISSN: 0009-921X

Sychter, C.J. & Engh, C.A. (1996). The influence of clinical factor on periprosthetic bone remodeling. *Clin Orthop Relat R*, 322, 285-292. ISSN: 0009-921X

Turner, M.J.; Clough, R.W.; Martin, M.C. & Topp, L.J. (1956). Stiffness and deflection analysis of complex structures. *J Aeronautical Society*, 23, 9, 805-823.

Weinans, H.; Huiskes, R. & Grootenboer, H.J. (1994). Effects of fit and bonding characteristics of femoral stems on adaptative bone remodelling. *J Biomech Eng,*116, 4, 393-400. ISSN: 0148-0731

White, A.A. & Panjabi, M.M. (1990). *Clinical Biomechanics of the Spine*, Lippincott Williams & Wilkins, Philadelphia. ISBN-10: 0397507208

Yaszemski, M.J.; White III, A.A., Panjabi, M.M. (2002). Biomechanics of spine, In: *Orthopaedic Knowledge Update: Spine 2*, Fardon, D.F. and Garfin, S.R. (Ed.), 17-26, Amer. Acad. Orth. Surgeons, Illinois

Zienkiewicz, O.C. & Morgan, K. (1983). *Finite element and approximation*, John Wiley & Sons, New York. ISBN 10: 0471982407

Zienkiewicz, O.C. (1967). *The finite element method in structural and continuum mechanics*, Prentice-Hall, New Jersey. ASIN: B000HF38VG

Finite Element Analysis

Edited by David Moratal

ISBN 978-953-307-123-7

Hard cover, 688 pages

Publisher Sciyo

Published online 17, August, 2010

Published in print edition August, 2010

Finite element analysis is an engineering method for the numerical analysis of complex structures. This book provides a bird's eye view on this very broad matter through 27 original and innovative research studies exhibiting various investigation directions. Through its chapters the reader will have access to works related to Biomedical Engineering, Materials Engineering, Process Analysis and Civil Engineering. The text is addressed not only to researchers, but also to professional engineers, engineering lecturers and students seeking to gain a better understanding of where Finite Element Analysis stands today.

InTech Europe

University Campus STeP Ri
Slavka Krautzeka 83/A
51000 Rijeka, Croatia
Phone: +385 (51) 770 447
Fax: +385 (51) 686 166
www.intechopen.com

InTech China

Unit 405, Office Block, Hotel Equatorial Shanghai
No.65, Yan An Road (West), Shanghai, 200040, China
中国上海市延安西路65号上海国际贵都大饭店办公楼405单元
Phone: +86-21-62489820
Fax: +86-21-62489821

IntechOpen